Experimental Study on Internal Porosity Structure of Chondrite Parent Bodies

Tomomi Omura[1], Akiko M. Nakamura[1]
[1]*Department of Planetology, Graduate School of Science, Kobe University*

Introduction: The porosity structure of chondrite parent bodies affects evolutionary path of the bodies. For instance, fractured region due to impact remains localized when the body has a porous internal structure [1][2]. The thermal evolution of chondrite parent bodies, coated with a thick, insulating, porous regolith has been shown to differ greatly from that of simple rocky bodies [3][4]. The porosity structure of chondrite parent bodies is determined by the soil pressure due to the equilibrium of self-gravity, centrifugal force, and tidal force, the presence of rocks, compaction by impacts [5][6], and compaction due to impact-induced vibrations. In particular, the porosity determined by soil pressure is the initial, most porous one when the centrifugal and tidal forces can be neglected. The porosity structure due to soil pressure can be estimated from the compaction properties of constituent materials of chondrite parent bodies. The compaction properties of the constituent materials should depend on their characteristics such as abundance of components which vary with chondrite type. In this study, we conducted compaction experiments of dust-beads mixtures and investigated effects of dust size and the dust-beads ratio on the compaction behavior. Then we calculated internal porosity structure of chondrite parent body using our experimental results.

Experiments: We used micrometer-sized dust particles and millimeter-sized solid beads as analogs of matrix and other chondrite components such as chondrules. We prepared dust-beads mixtures with different mixing ratio as samples. We poured the sample into a cylindrical container and the top part of the bed over the height of the container was leveled off. Then we compacted the sample using a piston fixed to the top plate of a compressive testing machine. The applied uniaxial pressure was up to ~10^7 Pa.

Results: Figure 1 shows results of experiments. The compaction properties of samples varied depending on both volume fraction of beads (f) and characteristics of dust particles. The filling factor of sample increased with volume fraction of beads under the same pressure except for the sample with f=0.78. Initially this sample had the highest filling factor but it was the least compressive because the amount of dust particles was not enough to fill the void space between beads particles. Compaction properties of different dust particles are also shown. The filling factor of almina sample which is the mixture of alumina particles with median diameter of 1.0 µm and alumina beads with diameter of 1 mm was lower than that of fly ash mixture. The alumina mixture was more compressible than fly ash mixture because the compaction properties of dust sample was mainly determined by particle size [7].

Calculation of model compaction curves: We calculated the pressure-filling factor relationship of mixtures as follows:

$\Phi_m(P)=\rho_m(P)/\rho_{m0}=\{(m_B/\rho_B)+(m_D/\rho_D)\}/\{(m_B/\rho_B(P))+(m_D/\rho_{\Phi D}(P))\}$,

where $\Phi_m(P)$ is the filling factor of mixture under the pressure P, ρ_m is the bulk density of mixture, ρ_{m0} is the true density of the mixture, $m_{B \text{ or } D}$ and $\rho_{B \text{ or } D}$ are the mass and grain density of beads and dust, respectively. $\rho_B(P)$ is the density of beads and we assumed ρ_B was not changed by the applied pressure ($\rho_B(P)=\rho_B$). $\rho_{\Phi D}(P)$ is the bulk density of dust layer with filling factor of Φ under the pressure P and we adopted experimental results of dust samples (f=1) for this value. Calculation results are also shown in Figure 1. Calculated compaction curves were consistent with the experimental results when the volume fraction of beads was smaller than ~0.6. In other words, the

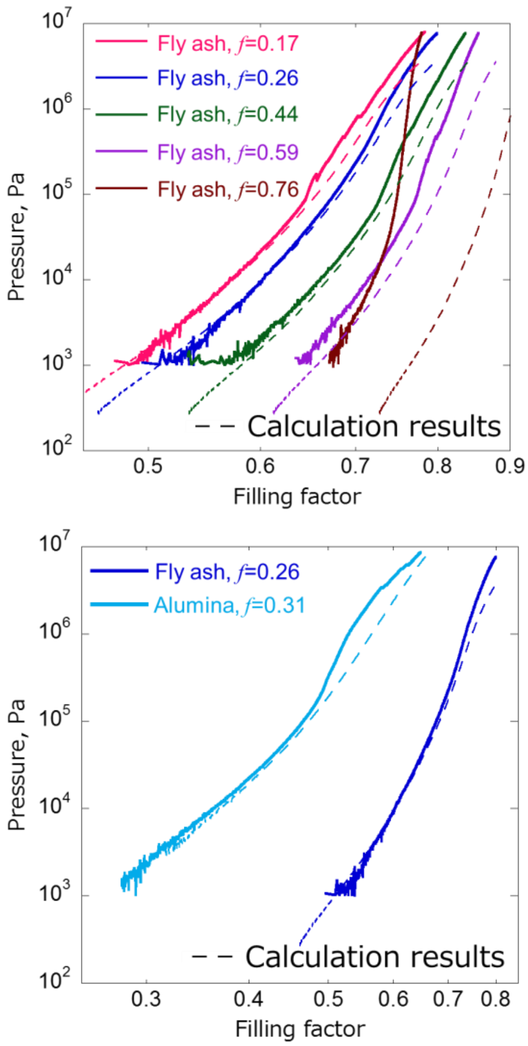

Figure 1. Results of experiments and calculation. Top: effect of volume fraction of beads. Samples were mixture of fly ash with median diameter of 4.8 µm and glass beads with diameter of 1 mm. Bottom: compaction properties of the mixture of fly ash and glass beads and the mixture of alumina particles and beads.

compaction property of mixture was determined by that of the dust sample when the ratio of the volume occupied by beads in the whole sample before compaction was smaller than ~0.4.

Calculation of porosity structure of chondrite parent body: We approximated the measured pressure-filling factor relationship of each sample with a power-law form (a modifying polytropic relationship). Fittings with power-law form were as good as fittings with different types of equations used for powder in previous studies. We calculated the porosity structure of chondrite parent body based on the approximated compaction properties of our samples with Lane-Emden equation (the same way described in [7]). Figure 2 shows results of calculation. The porosity of the body calculated from the compaction property of the alumina sample is higher than that calculated from that of fly ash sample. The porosity of ~0.2 is achieved in case of the body with radius of 30 km with the compaction property of a fly ash mixture sample (*f*=0.62). The porosity of CV chondrites (~0.2 [8]) can be achieved due to soil pressure in the parent body with 30 km radius when the compaction property of matrix can be described by that of fly ash. On the other hand, the bulk porosity of asteroid 253 Mathilde (0.53 [9]) is larger than that of the body with 30 km radius calculated with the compaction properties of fly ash samples, and similar to that calculated with that of an alumina mixture sample (*f*=0.31). Mathilde may consist of the materials with the compaction properties that can be described by alumina sample's ones. Further study is needed to investigate the effect of contained ice in the constituent materials of chondrite parent bodies on the compaction properties.

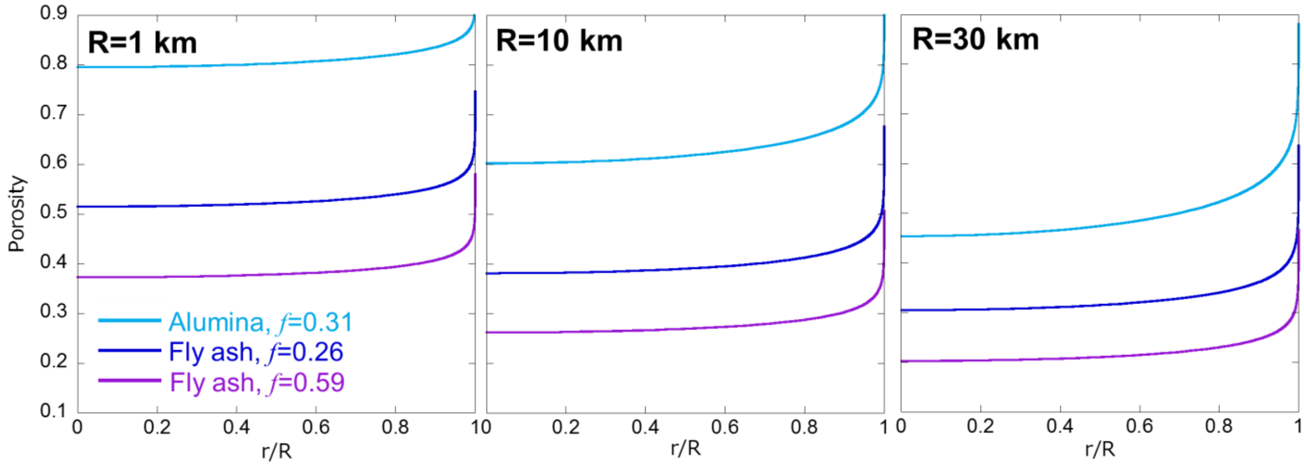

Figure 2. Calculated porosity structures of chondrite parent bodies.

References

[1] Love et al., 1993. Icarus 105, 216-224. [2] Asphaug et al., 1998. Nature 393, 437-440. [3] Akiridge, et al., 1998. Icarus 132, 185-195. [4] Henke et al., 2012. Astron. & Astrophys. 537, A45. [5] Beitz et al., 2013. Icarus 225, 558-569. [6] Forman et al., 2016. EPSL 452, 133-145. [7] Omura and Nakamura, 2018. Astrophys. J. 860, 123 (7pp). [8] Weisberg et al., 2006. In: D. S. Lauretta and H. Y. McSween Jr. (eds.), Meteorites and the Early Solar System II. University of Arizona Press, Tucson, 943 pp., p.19-52. [9] Baer et al., 2011. Astron. J. 141, 143 (12 pp).